Received: 7 December 2021 | Revised: 29 April 2022 | Accepted: 2 May 2022

DOI: 10.1111/jfpp.16730

Journal of Food Processing and Preservation | Institute of Food Science + Technology | WILEY

ORIGINAL ARTICLE

Impact of encapsulation techniques (drying methods and carrier materials) on the nutraceuticals release and absorption mechanism of mulberry leaf

William Tchabo[1,2] | Giscard Kuate Kaptso[3,4] | Guifeng Bao[1] | Kenuo Wang[1] | Newlove A. Afoakwah[5] | Carl Moses Mbofung[2] | Xiangyang Wang[1]

[1]School of Food Science and Biotechnology, Zhejiang Gongshang University, Hangzhou, P.R. China

[2]Department of Food Science and Nutrition, National Advanced School of Agro-Industrial Sciences (ENSAI), University of Ngaoundere, Ngaoundere, Cameroon

[3]Department of Social Economy and Family Management, Higher Technical Teacher's Training College (HTTTC), University of Buea, Kumba, Cameroon

[4]Department of Chemical Engineering, School of Chemical Engineering and Mineral Industries (EGCIM), University of Ngaoundere, Ngaoundere, Cameroon

[5]Department of Food Science and Technology, Faculty of Agriculture, Food and Consumer Sciences, University for Development Studies, Tamale, Ghana

Correspondence
William Tchabo, School of Food Science and Biotechnology, Zhejiang Gongshang University, Hangzhou 310018, P.R. China.
Email: williamtchabo@zjgsu.edu.cn; william.tchabo@univ-ndere.cm

Abstract

The current study assesses the impact of encapsulation techniques (drying methods and carriers) on the release and intestinal permeability of mulberry leaf nutraceuticals. The Papadopoulou model revealed that the significant delay ($p < .05$) in the release of nutraceuticals by encapsulation is mainly due to carrier material. This finding was corroborated by Hixson and Crowell's models which showed that the polymer matrix is a limiting factor of release rate. Furthermore, the efflux ratio showed that encapsulation, chiefly the carrier material led to a change in the intestinal absorption mechanism of biocompounds by shifting it from active transport to passive diffusion. Hence, sodium carboxymethyl cellulose was found to be more suitable for the control released of mulberry leaf nutraceuticals during in vitro digestion. While maltodextrin led to better apparent permeability of biocompounds. With regard to drying techniques, spray drying resulted in better control release and intestinal permeability of biocompounds than freeze drying.

Novelty impact statement: The significant delay in the release of nutraceuticals by encapsulation is mainly due to carrier material. Additionally, encapsulation, chiefly encapsulating agents led to a change in the intestinal absorption mechanism of biocompounds by shifting it from active transport to passive diffusion. With regard to drying techniques, spray drying resulted in better control release and intestinal permeability of biocompounds than of freeze drying.

1 | INTRODUCTION

Consumer awareness of the health benefits of food has sparked interest from food companies in using therapeutic herbal ingredients for the development of functional products (Espinosa-Páez et al., 2021). Amongst medicinal plants, mulberry (*Morus* spp.), chiefly its leaf is renowned for health-related properties due to its bioactive profile (He et al., 2020; Wen et al., 2019). Mulberry leaf extract has been extensively investigated this last decade regarding its antioxidant, neuroprotective, and anti-cancer effects among others (Dhiman et al., 2020; Wen et al., 2019). These findings add to evidence that mulberry leaf extract might be regarded as a polyvalent bioactive ingredient. However, bioactive molecules are unstable in liquid media, thus in order to prolongate the shelf-life and to ease their utilization by food companies, it is imperative to transform them into powder by removing solvents present in these extracts (Çam et al., 2014; Costamagna et al., 2017). Furthermore, bioactive components are highly susceptible to epimerization in alkaline pH and at a high temperature which alters their bioactivity (Costamagna et al., 2017). In addition, phenolic compounds have a very bitter and astringent taste, making it difficult to use them as a nutraceutical or to incorporate them directly into food products (Costamagna et al., 2017; Pasrija et al., 2015). This drawback from a food engineering point of view may be resolved through encapsulation, which

is an efficient process usually used for plant-based health products to preserve the bioactivity of their nutraceutical microparticles for long period (Tchabo et al., 2019).

The kinetics release of bioactive compounds is frequently discussed qualitatively by means of concentration-time profiles, especially with regard to the amount of biocompounds released after a precise time period. Nevertheless, more useful information may be gleaned using mathematical processing of kinetic data, which helps to assess the effect of food processes on the release mechanism (Flores & Kong, 2017). Hence, various semi-empirical, empirical, or theoretical models which take in consideration dissolution, diffusion, erosion, and swelling processes simultaneously have been developed to provide insight into the underlying release mechanism of entrapped biocompounds. However, some factors such as enzymes (amylase, pepsin, Pancreatin), electrolytes (sodium, calcium, sodium), bile salts, and pH may influence biocompounds to release from a matrix system.

Our research team previously investigated the encapsulation of bioactive compounds from mulberry leaf, which demonstrated that maltodextrin and sodium carboxymethyl cellulose coupled with spray-dry or freeze-dry could be employed efficiently in the production of a bioactive ingredient powder (Tchabo et al., 2019; Tchabo, Ma, Kaptso, et al., 2018). Nevertheless, as aforementioned encapsulated biomolecules must be released and absorbed throughout oral-gastrointestinal digestion to exert their putative health benefits. The release of biological compounds is dependent on the encapsulating conditions (Kanha et al., 2021), thereby affecting their absorption (González et al., 2020). However, there is a scarcity of studies on the impact of encapsulation techniques on the release, and the intestinal permeability of encapsulating biocompounds following in vitro oral-gastrointestinal digestion. Hence, considering the above-mentioned and the paucity of information on the effects of matrix composition, encapsulation techniques on the digestibility of encapsulated mulberry leaf extract powder, the present research aimed to assess the effects of drying methods and carrier materials on the in vitro oral-gastrointestinal release and ex vivo intestinal permeability of entrapped mulberry's leaf biocompounds. Thus, an in vitro digestion approach, including mouth and stomach phases, as well as an intestinal stage performed with everted gut sac model was used to investigate the impact of encapsulation techniques on the release and absorption mechanism of encapsulated and unencapsulated mulberry leaf bioactive components.

2 | MATERIALS AND METHODS

2.1 | Materials

Mulberry leaves (var. Nong Sang 14, *Morus alba* L.) were harvested in Jiangsu province, China from the Zhenjiang mulberry variety nursery base. The list of materials used is tabularized in Supporting Information S1.

2.2 | Methods

An aqueous mulberry leaf extract was obtained following the procedure reported by Tchabo, Ma, Kwaw, et al. (2018). Then, microencapsulated mulberry leaf extract powders were produced according to the method described by Tchabo, Ma, Kaptso, et al. (2018) and Tchabo et al. (2019), as summated in Supporting Information S2. In addition, lyophilized aqueous mulberry leaf extract without wall material was considered as a control. The unencapsulated and encapsulated mulberry leaf extract powders (MLEP) were kept at −29°C (within one week) before in vitro stimulated digestion.

2.3 | In vitro stimulated digestion

An in vitro stimulated oral-gastrointestinal digestion was performed according to Caicedo-Lopez et al. (2019) with slight modification as tabulated in Supporting Information S3. A written informed consent was signed by four participants, and the in vitro stimulated digestion was carried out following the guidelines, which involved humans or animals in accordance with the care and use of laboratory animals as implemented by the Provincial Health Institute.

2.4 | Nutraceutical release

The nutraceuticals release (N_{re}) of MLEP was related to the respective nutraceutical content of each sample, which was set at 100% and calculated as the percentage of bioactive compounds freeing at each preset time as follows:

$$N_{re} = 100 * \left[\left(C_{MLEP} - C_{PF}\right) / C_{MLEP}\right] \quad (1)$$

where C_{MLEP} is the nutraceutical content of MLEP and C_{PF} is the nutraceutical content of the pellet (oral, gastric, or intestinal) fraction.

The N_{re} data were fitted to various mathematical models employed in the literature (Díaz-Bandera et al., 2015; Kavousi et al., 2018) as follows:

$$\text{Papadopoulou model: } M_t / M_\infty = 1 - e^{-(kt)^{kl}} \quad (2)$$

$$\text{Zero} - \text{order model: } M_t / M_\infty = kt \quad (3)$$

$$\text{First} - \text{order model: } M_t / M_\infty = 1 - e^{-kt} \quad (4)$$

$$\text{Higuchi Model: } M_t / M_\infty = kt^{1/2} \quad (5)$$

$$\text{Hixson} - \text{Crowell model: } M_t / M_\infty = 1 - (1 - kt)^3 \quad (6)$$

$$\text{Korsmeyer} - \text{Peppas model: } M_t / M_\infty = kt^n \quad (7)$$

$$\text{Peppas} - \text{Sahlin model: } M_t / M_\infty = k_d t^m + k_r t^{2m} \quad (8)$$

$$\text{Kopcha model: } M_t / M_\infty = At^{1/2} + Bt \quad (9)$$

where M_t is the quantity of nutraceutical compounds released at time t; M_∞ is the maximum of nutraceuticals release; k is the release constant; k_l is the lag period; n is the release exponent; k_d is the diffusion constant; k_r is the relaxation constant; m is the Fickian diffusion exponent; A is the diffusional constant and B is the dissolution or erosional constant.

2.5 | Intestinal permeability assays

2.5.1 | Permeability coefficients

The permeability coefficients were computed according to Caicedo-Lopez et al. (2019), based on the equations as follows:

$$P_{app} = (dQ/dt)(1/AC_0) \tag{10}$$

$$P_{app\ net} = \left|P_{app\ B\ to\ A} - P_{app\ A\ to\ B}\right| \tag{11}$$

$$ER = P_{app\ B\ to\ A} / P_{app\ A\ to\ B} \tag{12}$$

where $P_{app}\,(cm/s)$ is the apparent permeability coefficient, $dQ/dt\,(g/s)$ is the amount of nutraceutical transported across the intestinal membrane per unit time $A\,(cm^2)$ represents the intestinal mucosal area surface available for permeation, $C_0\,(mg/g\ db)$ is the initial content of nutraceuticals at the apical side (outside the everted gut sac), $P_{app\ B\ to\ A}\,(cm/s)$ is the apparent permeability coefficient from the basolateral to apical, $P_{app\ A\ to\ B}\,(cm/s)$ is the apparent permeability coefficient from the apical to basolateral, $P_{app\ net}$ is the and ER is the efflux ratio.

2.5.2 | Predictive permeability screening

The predictive permeability and intuitive intestinal absorption prediction of MLPE nutraceuticals were assessed according to Luzardo-Ocampo et al. (2020). The nutraceuticals SMILES files obtained from PubChem database (https://pubchem.ncbi.nlm.nih.gov/) were used to determine the predicted bioavailability radar, the probabilities of nutraceuticals to cross the epithelial barrier in the caco-2 cells monolayer model, and their reported human intestinal absorption using the admetSAR 2.0 software (http://lmmd.ecust.edu.cn/admetsar2). The "Boiled Egg" diagram was carried out from the WLOGP (Wildman & Crippen atomistic interpretation of the fragmental system) versus TPSA (topological polar surface area) plots using the SwissADME (http://www.swissadme.ch/index.php).

2.6 | Nutraceutical's characterization

The nutraceuticals were identified and quantified following the reported procedure of Tchabo, Ma, Kwaw, et al. (2018) using a high-performance liquid chromatography Shimadzu apparatus (Kyoto, Japan) compose of a photodiode array detector SPD-M20A, pump LC-20AB, degasser DGU-20A5R, autosampler SIL 20AC, column oven CTO- 20AC, system controller SCL-10A, LC Solution software, and a 250×4.6 mm, 5 μm C18 column ZORBAX-SB (Agilent, Santa Clara, USA). The contents were expressed in mg of nutraceutical per g of the dry base. The biocomponents identified and quantified were clustered as the sum of flavonols (∑FC), the sum of phenolic acids (∑PAC) and the sum of nutraceuticals (∑NC).

2.7 | Statistical analysis

All the in vitro and ex vivo experiments, as well as assays, were performed thrice. The statistical difference among means was assessed by means of Tukey–Kramer test at a 5% significance level using Minitab 19 (Minitab Inc., 296 Pennsylvania, USA). The release kinetic data were fitted with OriginPro 2020 software (OriginLab, Northampton, USA).

3 | RESULTS AND DISCUSSION

3.1 | Mathematical modeling of in vitro release kinetics of nutraceuticals

3.1.1 | Nutraceutical's release

In order to assess the impact of encapsulation on the release behavior of biocompounds from MLEP as a function of carrier materials and drying techniques, a modified first-order kinetic modeling based on Weibull distribution proposed by Papadopoulou et al. (2006) was performed. That model has been employed by Díaz-Bandera et al. (2015) to evaluate the effect of encapsulating agents on the release kinetics of polyphenols and dissolution of spray-dried *Hibiscus sabdariffa* L. extract. The high values (Adj-$R^2 > .88$) of the coefficient of determination and low values of the standard error (SE < 0.07) for each MLEP tabulated in Table 1, revealed that the nutraceuticals release process obeys the Weibull model with the first-order probabilistic forecast. The Papadopoulou model outcomes (Table 1) highlighted significant differences in the behavior of MLEPs during bioactive compounds release. With regard to the unencapsulated MLEP (Supporting Information S4), it can be seen that the release of ∑NC, at the steady-state (M_∞), attained a maximum of 90.81% (with 97.65% for ∑PAC, 88.03% for ∑FC, for 97.23% for DNJ, and 98.85% for GABA). This can be attributed to its dissolution in the digestion fluids as stated by Díaz-Bandera et al. (2015). Moreover, the release behavior of MLEPs might be ascribed to water-microparticles interaction due to the amorphous physical condition of MLEP that led to the enhancement of its solubility (Zokti et al., 2016). Furthermore, it was noted that at M_∞, the encapsulated samples released significantly less nutraceuticals ($p < .05$) than the unencapsulated sample

TABLE 1 Kinetic parameters of Papadopoulou model obtained from the release curves of nutraceuticals of mulberry leaf extract powder

Nutraceuticals	MLEP	Adj R^2	M_∞	SE M_∞	k_p	SE k	k_L	SE k_L
CHA	FD	0.985	9.7E+1^a	3.5E-3	2.7E-2^a	1.8E-3	6.3E-1^b	3.3E-2
	FDMD	0.992	8.2E+1^c	3.2E-2	1.1E-2^b	3.7E-4	7.5E-1^b	3.1E-2
	SDMD	0.995	8.3E+1^b	3.7E-2	1.1E-2^b	2.8E-4	7.6E-1^b	2.6E-2
	FDCMC	0.979	7.2E+1^e	9.4E-3	4.5E-3^c	1.5E-4	1.4E+0^a	9.4E-2
	SDCMC	0.965	7.5E+1^d	2.0E-3	4.6E-3^c	1.8E-4	1.5E+0^a	1.3E-1
CA	FD	0.991	9.9E+1^a	1.1E-3	3.5E-2^a	1.9E-3	6.0E-1^b	2.4E-2
	FDMD	0.990	8.0E+1^c	6.1E-2	1.2E-2^b	4.5E-4	7.2E-1^b	3.3E-2
	SDMD	0.996	8.4E+1^b	1.0E-2	1.2E-2^b	2.6E-4	7.5E-1^b	2.1E-2
	FDCMC	0.969	7.6E+1^e	2.3E-2	4.6E-3^c	2.1E-4	1.1E+0^a	8.7E-2
	SDCMC	0.934	8.0E+1^d	5.2E-3	4.6E-3^c	2.9E-4	1.2E+0^a	1.3E-1
∑PAC	FD	0.988	9.8E+1^a	2.7E-3	3.0E-2^a	1.8E-3	6.2E-1^b	2.9E-2
	FDMD	0.992	8.1E+1^c	4.1E-2	1.1E-2^b	3.9E-4	7.4E-1^b	3.1E-2
	SDMD	0.995	8.3E+1^b	2.9E-2	1.1E-2^b	2.6E-4	7.6E-1^b	2.3E-2
	FDCMC	0.977	7.4E+1^e	1.4E-2	4.5E-3^c	1.6E-4	1.3E+0^a	8.9E-2
	SDCMC	0.958	7.7E+1^d	3.0E-3	4.6E-3^c	2.0E-4	1.4E+0^a	1.3E-1
K3M	FD	0.990	9.3E+1^a	2.4E-2	3.0E-2^a	1.6E-3	4.8E-1^b	1.7E-2
	FDMD	0.993	7.4E+1^c	4.7E-2	9.1E-3^b	2.9E-4	6.2E-1^b	2.2E-2
	SDMD	0.998	7.6E+1^b	2.3E-2	8.7E-3^b	1.5E-4	6.0E-1^b	1.1E-2
	FDCMC	0.973	5.7E+1^e	6.6E-3	3.3E-3^c	1.8E-4	1.2E+0^a	9.0E-2
	SDCMC	0.960	6.0E+1^d	2.4E-2	3.6E-3^c	1.9E-4	1.4E+0^a	1.2E-1
K3R	FD	0.989	9.1E+1^a	2.6E-2	2.7E-2^a	1.5E-3	4.8E-1^b	1.7E-2
	FDMD	0.997	7.2E+1^c	5.5E-2	6.5E-3^b	1.2E-4	6.4E-1^b	1.3E-2
	SDMD	0.989	7.8E+1^b	2.8E-2	7.2E-3^b	2.7E-4	6.2E-1^b	2.6E-2
	FDCMC	0.963	5.0E+1^e	5.2E-2	2.6E-3^c	2.1E-4	1.1E+0^a	8.8E-2
	SDCMC	0.937	5.4E+1^d	1.0E-2	2.8E-3^c	2.6E-4	1.1E+0^a	1.2E-1
K3G	FD	0.994	8.8E+1^a	4.0E-2	2.5E-2^a	9.6E-4	4.3E-1^b	1.0E-2
	FDMD	0.997	7.3E+1^c	5.2E-2	7.8E-3^b	1.7E-4	6.1E-1^b	1.5E-2
	SDMD	0.997	7.5E+1^b	4.3E-2	7.7E-3^b	1.5E-4	5.6E-1^b	1.1E-2
	FDCMC	0.976	5.5E+1^e	3.9E-2	3.0E-3^c	1.7E-4	1.1E+0^a	7.1E-2
	SDCMC	0.962	5.9E+1^d	2.2E-2	3.4E-3^c	2.0E-4	1.3E+0^a	1.1E-1
K7G	FD	0.988	9.0E+1^a	9.5E-3	3.2E-2^a	1.8E-3	4.5E-1^b	1.6E-2
	FDMD	0.998	7.8E+1^c	3.4E-2	8.6E-3^b	1.4E-4	6.1E-1^b	1.1E-2
	SDMD	0.996	7.8E+1^b	9.4E-3	8.3E-3^b	2.0E-4	5.5E-1^b	1.4E-2
	FDCMC	0.966	6.0E+1^e	3.9E-2	3.3E-3^c	2.1E-4	1.0E+0^a	8.3E-2
	SDCMC	0.959	6.1E+1^d	9.4E-3	3.3E-3^c	2.3E-4	1.0E+0^a	9.1E-2
Q3R	FD	0.980	8.1E+1^a	6.8E-3	1.3E-2^a	8.4E-4	4.4E-1^b	2.1E-2
	FDMD	0.993	6.4E+1^c	9.2E-3	5.3E-3^b	1.8E-4	6.1E-1^b	2.2E-2
	SDMD	0.998	6.7E+1^b	1.2E-2	5.4E-3^b	8.9E-5	6.2E-1^b	1.1E-2
	FDCMC	0.974	6.6E+1^e	3.0E-2	4.2E-3^b	1.0E-4	2.4E+0^a	1.6E-1
	SDCMC	0.973	7.4E+1^d	1.7E-3	4.5E-3^b	9.0E-5	2.8E+0^a	1.9E-1
Q3M	FD	0.987	8.6E+1^a	3.2E-2	1.8E-2^a	9.6E-4	5.0E-1^b	2.0E-2
	FDMD	0.992	6.8E+1^c	3.6E-2	6.7E-3^b	2.2E-4	6.4E-1^b	2.5E-2
	SDMD	0.996	7.0E+1^b	3.8E-2	6.9E-3^b	1.5E-4	6.4E-1^b	1.6E-2
	FDCMC	0.989	3.7E+1^e	3.5E-2	2.0E-3^c	1.1E-4	1.1E+0^a	5.2E-2
	SDCMC	0.984	4.1E+1^d	8.0E-3	2.4E-3^c	1.3E-4	1.3E+0^a	7.2E-2

TABLE 1 (Continued)

Nutraceuticals	MLEP	Adj R^2	M_∞	SE M_∞	k_p	SE k	k_L	SE k_L
Q3G	FD	0.989	8.3E+1^{a}	4.4E-2	1.7E-2^{a}	8.0E-4	4.2E-1^{b}	1.3E-2
	FDMD	0.992	6.6E+1^{c}	5.1E-2	6.1E-3^{b}	2.1E-4	6.2E-1^{b}	2.4E-2
	SDMD	0.997	6.8E+1^{b}	2.5E-2	6.1E-3^{b}	1.2E-4	6.0E-1^{b}	1.3E-2
	FDCMC	0.986	4.4E+1^{e}	2.4E-2	2.5E-3^{c}	1.3E-4	1.2E+0^{a}	6.3E-2
	SDCMC	0.980	4.5E+1^{d}	3.9E-3	2.6E-3^{c}	1.5E-4	1.3E+0^{a}	7.8E-2
∑FC	FD	0.991	8.8E+1^{a}	3.0E-2	2.3E-2^{a}	1.1E-3	4.6E-1^{b}	1.5E-2
	FDMD	0.996	7.1E+1^{c}	4.4E-2	7.2E-3^{b}	1.7E-4	6.2E-1^{b}	1.7E-2
	SDMD	0.999	7.3E+1^{b}	3.0E-2	7.2E-3^{b}	8.6E-5	6.0E-1^{b}	7.9E-3
	FDCMC	0.977	5.0E+1^{e}	3.2E-2	2.8E-3^{c}	1.6E-4	1.2E+0^{a}	7.7E-2
	SDCMC	0.967	5.3E+1^{d}	1.3E-2	3.1E-3^{c}	1.8E-4	1.4E+0^{a}	1.1E-1
DNJ	FD	0.990	9.7E+1^{a}	1.9E-3	2.9E-2^{a}	1.5E-3	5.3E-1^{c}	1.9E-2
	FDMD	0.997	8.5E+1^{c}	3.1E-3	1.2E-2^{b}	2.6E-4	7.3E-1^{bc}	1.9E-2
	SDMD	0.999	8.6E+1^{b}	3.6E-2	1.2E-2^{b}	1.8E-4	6.9E-1^{c}	1.1E-2
	FDCMC	0.950	7.7E+1^{e}	1.6E-2	4.5E-3^{c}	2.5E-4	1.2E+0^{ab}	1.2E-1
	SDCMC	0.885	8.4E+1^{d}	8.0E-3	4.8E-3^{c}	3.5E-4	1.3E+0^{a}	1.9E-1
GABA	FD	0.981	9.9E+1^{a}	1.8E-3	3.5E-2^{a}	2.8E-3	6.6E-1^{b}	4.2E-2
	FDMD	0.996	8.5E+1^{c}	3.4E-2	1.3E-2^{b}	3.3E-4	7.4E-1^{b}	2.2E-2
	SDMD	0.998	8.7E+1^{b}	2.2E-2	1.3E-2^{b}	2.1E-4	7.1E-1^{b}	1.3E-2
	FDCMC	0.974	6.7E+1^{e}	2.6E-2	4.0E-3^{c}	1.9E-4	1.1E+0^{a}	8.1E-2
	SDCMC	0.957	6.9E+1^{d}	1.8E-2	4.0E-3^{c}	2.3E-4	1.2E+0^{a}	1.0E-1
∑NC	FD	0.990	9.1E+1^{a}	2.2E-2	2.5E-2^{a}	1.3E-3	5.0E-1^{b}	1.7E-2
	FDMD	0.995	7.4E+1^{c}	4.1E-2	8.4E-3^{b}	2.2E-4	6.6E-1^{b}	2.1E-2
	SDMD	0.999	7.7E+1^{b}	3.0E-2	8.5E-3^{b}	1.0E-4	6.5E-1^{b}	9.5E-3
	FDCMC	0.977	5.7E+1^{e}	2.7E-2	3.2E-3^{c}	1.6E-4	1.2E+0^{a}	8.0E-2
	SDCMC	0.962	6.0E+1^{d}	1.0E-2	3.5E-3^{c}	1.9E-4	1.4E+0^{a}	1.1E-1

For the same nutraceutical components, means in the same column with different letter (a–e) are significantly different at $p < .05$ (Tukey's test).
Abbreviations: Adj R^2, ajusted R-square; CA, caffeic acid; CHA, chlorogenic acid; DNJ, 1-deoxynojirimycin; FD, freeze dry; FDCMC, freeze dried with sodium carboxymethyl cellulose; FDMD, freeze dried with maltodextrin; GABA, gamma-aminobutyric acid; k_L, lag period; k_p, release constant rate; K3M, kaempferol-3-(6-malonylglucoside); K3R, kaempferol-3-(6-rhamnosylglucoside); K3G, kaempferol-3-glucoside; K7G, kaempferol-7-O-glucoside; M_∞- SE, standard error; MLEP, mulberry leaf encapsulated powder; SDCMC, spray dried with sodium carboxymethyl cellulose; SDMD, spray dried with maltodextrin; Q3G, quercetin-3-O-glucoside; Q3M, quercetin-3-(6-malonylglucoside); Q3R, quercetin-3-rutinose; ∑ FC, sum of flavonol components; ∑ PAC, sum of phenolic acid components; ∑ NC, sum of nutraceutical components.

(Table 1), depicting the capacity of the encapsulation process to withhold the biomolecules of MLEP. Additionally, with respect to the encapsulating conditions, the low M_∞ values observed for sodium carboxymethyl cellulose and spray-dry highlighted their better ability to retain nutraceuticals as compared to maltodextrin and freeze dry. Taking into account the constant rate (k_p), it was observed that the unencapsulated sample showed the lowest k_p value followed by statistically similar groups formed by encapsulated samples with maltodextrin, and then samples embedded in sodium carboxymethyl cellulose (Table 1). Furthermore, with reference to the *Lag* period (k_L), there was no statistical differences ($p < .05$) between unencapsulated samples and entrapped samples with maltodextrin. On the contrary, encapsulated samples with sodium carboxymethyl cellulose showed the highest k_L. This behavior of carrier materials could be due to the hydrophilic nature, and high solubility of maltodextrin leading to the fast release of nutraceuticals. However, the high molecular weight and low water solubility of carboxymethyl cellulose may have caused the delay in the release of bioactive components. This trend has been reported by Zokti et al. (2016). However, drying techniques were found to have no significant impact ($p < .05$) on k_p and k_L depending on the type of support materials applied.

3.1.2 | In vitro release mechanism

A biphasic release behavior was observed in the release profile graphs (Supporting Information S4) for all the systems studied. The first zone (oral phase) corresponded to an initial rapid release of the uncovered nutraceuticals (superficial) on the surface of the encapsulated microparticles, and the inhomogeneous distribution of particle size of unencapsulated sample throughout the oral digestion. The

second zone (gastric and intestinal phases) presented a gradual release of nutraceuticals with time until attained a plateau. As stated by Madene et al. (2006), the release of a biomolecule from a matrix is governed by the physicochemical properties of the core and carriers (molecular weight, polarity, and chemical functionality), as well as the encapsulation techniques (Madene et al., 2006), that influence the polymer swelling, and plasticization leading to diffusion and erosion phenomena. This induces the freeing of compounds into the outer solution till the thermodynamic equilibrium is reached (Serrano-Cruz et al., 2013). Hence, in order to assess the effect of encapsulation conditions on the controlled release of nutraceutical components from MLEPs, the gastric and intestinal release kinetic data were fitted to various mathematical models in order to determine the release mechanisms.

The rank model app in Originpro that allow to compare multiple fitting functions in order to identify the best fitting model based on five statistical measures (adjusted R^2, residual sum of squares, reduced chi-Square, Akaike information criterion, Bayesian information criterion) was used to select the release model, that best fitted the experimental data. From the results of Supporting Information S5, it was found that the most suitable models to describe the release kinetics of MLPE's nutraceuticals during gastric digestion were as follows: Korsmeyer-Peppas > Peppas-Sahlin > Kopcha for unencapsulated sample, Peppas-Sahlin > Higuchi > Korsmeyer-Peppas for samples encapsulated with maltodextrin and Kopcha > Korsmeyer-Peppas > first-order for samples encapsulated with sodium carboxymethyl cellulose. Meanwhile, for the intestinal digestion phase, the models which fitted the best were as follows: Korsmeyer-Peppas > Kopcha > Peppas-Sahlin; Higuchi > Kopcha > Korsmeyer-Peppas; and Zero order > Kopcha > Korsmeyer-Peppas, for unencapsulated sample, encapsulated samples with maltodextrin, and samples encapsulated with sodium carboxymethyl cellulose, respectively.

It was observed that release data of all the MLEP (Supporting Information S5) were well fitted (adj-R^2 > .82) with Korsmeyer-Peppas model. Thus, according to the Supporting Information S6, the n value of the Korsmeyer-Peppas model outcome (Supporting Information S7), are characteristic of pseudo-Fickian diffusion (for the unencapsulated sample at gastric phase), Fickian diffusion (for samples encapsulated with maltodextrin at the gastric and intestinal phase), non-Fickian diffusion (for the unencapsulated sample at intestinal stage and samples encapsulated with sodium carboxymethyl cellulose at gastric phase), and case II transport (for samples encapsulated with sodium carboxymethyl cellulose at intestinal phase). Given the fact that Korsmeyer-Peppas model gives little cognizance about the freeing mechanism (Rezaei et al., 2016), the computed Peppas-Sahlin (adj-R^2 > .81 for all MLEP), and Kopcha (adj-R^2 > .83 for all MLEPs) models revealed the occurrence of relaxational and erosion mechanism in addition to the Fickian diffusion. As seen in Supporting Information S7, k_d was higher than k_r, which indicated that the biocompounds released were chiefly controlled by Fickian diffusion and lesser dependent on the polymer relaxation. This might be attributed to the high porosity of MLEPs (Tchabo et al., 2019; Tchabo, Ma, Kaptso, et al., 2018). Bacaita et al. (2014) also noted a similar finding. Furthermore, the values of A larger than B (Supporting Information S7) buttressed the preponderance of diffusion relative to the erosion process, except for intestinal digestion of samples encapsulated with sodium carboxymethyl cellulose where the erosion of polymer chain was more pronounced ($A < B$). On the other hand, the Higuchi model that allowassessing the pure Fickian release was well fitted with MLEPs (adj-R^2 > .76) except for the gastric digestion of the unencapsulated sample (adj-R^2 < .58). This bolstered the assumption of a strong influence of Fickian diffusion in the release mechanism of nutraceuticals from MLEPs. A similar pattern has been observed by Trevisol et al. (2020). Furthermore, the Hixson and Crowell model mathematically described well the release of nutraceuticals from MLEPs (adj-R^2 > .72), excluding that of the gastric digestion of unencapsulated samples and intestinal digestion of encapsulated samples with maltodextrin (adj-R^2 < .63), thus assuming that the rate of dissolution through the polymer matrix is a limiting factor (Malekjani & Jafari, 2020). From the hypothesis of the influence of polymer matrix on dissolution rate, the first-order modeling kinetic released of these samples (adj-R^2 > .78), showed that the driving forces of the freeing process depend on the biocompounds concentration (Malekjani & Jafari, 2020). However, the high correlation coefficients (adj-R^2 > .68) of the zero model at the gastric stage (for samples encapsulated with sodium carboxymethyl cellulose) and the intestinal stage (for unencapsulated samples and samples encapsulated with sodium carboxymethyl cellulose) indicated a reduction in the attractive forces between polymer chains. This might be due to the influence of swelling and polymeric hydration on biomolecule release that may be related to matrix erosion (Pereira Camelo et al., 2016). Thereby corroborating the outcomes of the Kopcha model.

3.2 | Intestinal absorption

3.2.1 | Ex vivo intestinal permeation

Intestinal permeability is a crucial parameter that assesses the capacity of a biomolecule to cross the intestinal barrier, thus reflecting its absorption ability from both the apical side (intestinal lumen) to the basolateral side (bloodstream). From the apical to basolateral side (Supporting Information S8), the nutraceuticals exhibited a decrease in absorptive permeability over the time with their upmost $P_{app\ A\ to\ B}$ at 15 min, except K7G and K3R of the unencapsulated sample, which had their highest $P_{app\ A\ to\ B}$ at 30 and 60 min, respectively. Furthermore, phenolic acids presented the uppermost $P_{app\ A\ to\ B}$ (18.73 to 23.11 $\times 10^{-6}$ cm/s), followed by DNJ (16.12 to 24.41 $\times 10^{-6}$ cm/s), then GABA (4.49 to 16.29 $\times 10^{-6}$ cm/s) and flavonols (5.51 to 12.05 $\times 10^{-6}$ cm/s). As stated by Herrera-Cazares et al. (2017), the low intestinal permeability of flavonols to blood flux could be ascribed to their hydrophobic character. Moreover, according to Caicedo-Lopez et al. (2019) the differences in the $P_{app\ A\ to\ B}$ of biocompounds may be related to their intrinsic solubility in aqueous media. Furthermore, in line with our results, previous

authors (Aguillón-Osma et al., 2019; Caicedo-Lopez et al., 2019; Rastogi & Jana, 2016; Tian et al., 2009) reported high permeation in the absorptive direction for phenolic acids and flavonols. Besides, the Permeation of ∑NC in the B to A direction significantly ($p < .05$) reduced throughout intestinal digestion (Supporting Information S9), thus suggesting a stabilization of nutraceuticals diffusion from basolateral to the apical side of the duodenum. For individual biocompounds, the highest intestinal transport in the B to A direction was mostly performed in the first 15 min (Supporting Information S9) with the exception of K7G (at 30 min for spray-dry encapsulated samples with CMC), DNJ, and GABA (at 30 min for unencapsulated sample) as well as Q3G (at 60 min for all MLEPs). It is noteworthy that some components such as K3R (from 60 to 120 min for all MELPs), Q3R (from 60 to 120 min for unencapsulated samples and encapsulated samples with MD, and at 120 min for encapsulated samples with CMC), Q3M (from 60 to 120 min for unencapsulated sample, and from 30 to 120 for encapsulated samples), and Q3G (from 15 to 30 min for all MELPs) did not diffuse from basolateral to the apical side. Furthermore, it was observed that at the end of the intestinal phase, the transport rate was chiefly in the A to B than the B to A direction, suggesting that absorption of nutraceuticals was performed in the late stage of duodenal digestion. Similar trend has been reported by Herrera-Cazares et al. (2017). Additionally, considering precedents rapports (Caicedo-Lopez et al., 2019; Campos-Vega et al., 2015; Quilaqueo et al., 2019) concerning the permeation speed of pure biocomponents, the $P_{app\ net}$ values of ∑NC from MLEPs (Supporting Information S10) have been found to be above 1×10^{-6} cm/s, a common cutoff advocating a high permeation capacity (Feng et al., 2019), which suggest that they could be well absorbed in human beings (Villela-Castrejón et al., 2017). It was also noted that the $P_{app\ net}$ of the evaluated compounds (Supporting Information S10) tends to decrease over time. Further, it was noted that encapsulation of MLEPs led to a significant decrease ($p < .05$) in $P_{app\ net}$ (Supporting Information S10). Some authors have reported an increase in permeability of green tea catechin nano-encapsulated with zein using the electrospraying technique (Bhushani et al., 2017), astaxanthin encapsulated with whey protein through an emulsification-evaporation technique (Shen et al., 2018), cyanidin-3-O-glucoside encapsulated by composite nanogel (Feng et al., 2019). While other researchers have observed a decrease in the permeability of liposome-encapsulated rosemary phytochemicals (Pérez-Sánchez et al., 2017), olive pomace polyphenols were encapsulated with cyclodextrin by lyophilization (Radić et al., 2020). These contradictory results on the notion of improving the permeability of biocomponents by encapsulation deserve further study. However, as stated by previous authors (González et al., 2019; Heep et al., 2019), several factors such as carrier materials, molecule size, components content, particle size, and solubility of food matrix alter the intestinal transport of biocompounds. Herein, the high permeability of compounds encapsulated with maltodextrin compared to those with sodium carboxymethyl cellulose may be due to the inherent solubility of the encapsulating agent, while the higher permeability of spray-dry samples than that of freeze-dry samples could be attributed to the impact of drying methods on particle size. As earlier reported (Tchabo et al., 2019; Tchabo, Ma, Kaptso, et al., 2018), MLEPs encapsulated with maltodextrin have greater solubility than MLEPs encapsulated with sodium carboxymethyl cellulose, whereas the atomization of MLEP leads to smaller particle size than that of lyophilization. Besides, the ER has been employed in the literature (Aguillón-Osma et al., 2019; Luzardo-Ocampo et al., 2017; Quilaqueo et al., 2019) to predict the absorption mechanism of biocompounds by determining if it is active (ER < 0.5 or ER > 2.0) or passive (0.5 < ER < 2.0). Based on these criteria, it was found that non-encapsulated biomolecules were transported into the small intestine by active mechanism (Supporting Information S11) while encapsulated biocompounds were able to permeate through the small bowel by passive diffusion. These differences in the mechanism might be attributed to carrier materials, which could facilitate the transport of nutraceuticals during their absorption. As stated by some researchers (Berkane et al., 2005; Kullman et al., 2002) maltoporin a membrane protein is a passive specific channel for the maltodextrin uptake. Furthermore, the lowest efflux ratios reported at 120 min indicate that an extended intestinal passage led to better intestinal absorption of nutraceuticals with a reduction of their intestinal lumen return. A similar observation was made by Quilaqueo et al. (2019).

3.2.2 | Intuitive prediction of absorption and permeability

The $P_{app\ net}$ values of MLEP's nutraceuticals were found to be higher than that reported in the Caco-2 cell predictive model (Table 2). This slight difference found in this study could be attributed to the interactions between these biocompounds and the food matrix since the biocompounds permeability in the Caco-2 cell predictive model has been performed using pure components. A similar finding has been made by Caicedo-Lopez et al. (2019) regarding the permeation of phenolic compounds from *Moringa oleifera* leaves. Furthermore, the bioavailability radar of each nutraceutical representing the descriptors for polarity, lipophilicity, saturation, solubility, flexibility, and size was illustrated in Figure 1. As stated by Luzardo-Ocampo et al. (2020), the pink color portrays the oral limits of the five properties, which are within the limits of the size (molecular weight) of 150–500, number of rotatable bonds (flexibility) 0–9, polarity 20–130, log P − 0.7–5, and water solubility score 1–3 (where 1 is the highest and 5 is the lowest). Except for the IS (for CA) and PO (for CHA, K3M, K3R K3G, K7G, Q3R, Q3M, and Q3G), all the evaluated bioactive compounds fitted within the limits of other parameters. Moreover, DNJ, CHA, K7G, and K3G presented a different polarity, explaining the different trends observed for these biomolecules in the "Boiled Egg" diagram. Additionally, the white region of the "Boiled Egg" diagram is associated with a higher probability of passive intestinal absorption. Hence, the location of DNJ, CHA, K7G, and K3G outside this zone is an indicator of another type of transport mechanism; even though, the "Boiled Egg" diagram does not

TABLE 2 Intuitive prediction of absorption and permeability of nutraceuticals from mulberry leaf extract powders

	Obtained Papp ($\times 10^{-6}$ cm/s) of MLEP and predicted ADMET Caco-2 permeability ($\times 10^{-6}$ cm/s)						Prediction of the absorption's probability		
	In vitro intestinal digestion								
Nutraceuticals	FD	FDMD	SDMD	FDCMC	SDCMC	Caco-2 model	Human intestinal absorption	Caco-2 permeability	Human oral bioavailability
Phenolic acids									
CHA	8.73–20.58	3.01–9.93	3.95–12.65	1.96–6.39	2.68–7.39	0.2441	0.9020	0.9230	0.7000
CA	4.71–18.07	1.58–7.02	2.36–11.51	1.01–4.27	1.83–7.70	2.2310	0.9645	0.5000	0.6429
Flavonols									
K3M	4.07–6.81	1.27–4.05	2.26–6.66	0.63–1.98	1.11–2.97	0.1085	0.6465	0.9224	0.7000
K3R	7.58–13.80	1.25–6.16	2.67–8.91	0.41–3.07	1.18–4.84	0.4882	0.7512	0.9122	0.7143
K3G	5.30–10.85	1.11–3.34	2.37–7.16	0.20–2.38	1.06–4.14	0.1386	0.6347	0.9102	0.7714
K7G	6.86–12.00	1.06–4.86	2.36–7.76	0.18–1.27	0.44–3.80	0.1386	0.6347	0.9536	0.7714
Q3R	1.85–7.64	1.09–2.15	1.54–3.86	0.12–0.67	0.36–1.10	0.2235	0.7322	0.9269	0.7429
Q3M	2.02–11.27	1.06–3.62	1.82–6.21	0.42–1.52	0.55–1.97	0.1085	0.6510	0.9237	0.6714
Q3G	1.13–8.90	0.44–6.38	0.65–8.65	0.14–2.49	0.18–3.04	0.1386	0.6468	0.9010	0.7286
Other nutraceuticals									
DNJ	5.14–23.99	1.65–6.86	2.87–10.34	1.04–5.52	1.65–6.57	0.7523	0.7392	0.9638	0.6571
GABA	3.18–8.35	0.40–1.90	1.81–7.16	0.19–1.36	0.47–2.67	7.6948	0.8297	0.5000	0.6571

Abbreviations: ADMET, Absorption, Distribution, Metabolism, Excretion and Toxicity; CA, caffeic acid; CHA, chlorogenic acid; FD, freeze dry; FDCMC, freeze dried with sodium carboxymethyl cellulose; FDMD, freeze dried with maltodextrin; DNJ, 1-deoxynojirimycin; GABA, gamma-aminobutyric acid; K3M, kaempferol-3-(6-malonylglucoside); K3R, kaempferol-3-(6-rhamnosylglucoside); K3G, kaempferol-3-glucoside; K7G, kaempferol-7-O-glucoside; Q3R, quercetin-3-rutinose; Q3M, quercetin-3-(6-malonylglucoside); Q3G, quercetin-3-O-glucoside; MLEP, mulberry leaf encapsulated powder; SDCMC, spray dried with sodium carboxymethyl cellulose; SDMD, spray dried with maltodextrin.

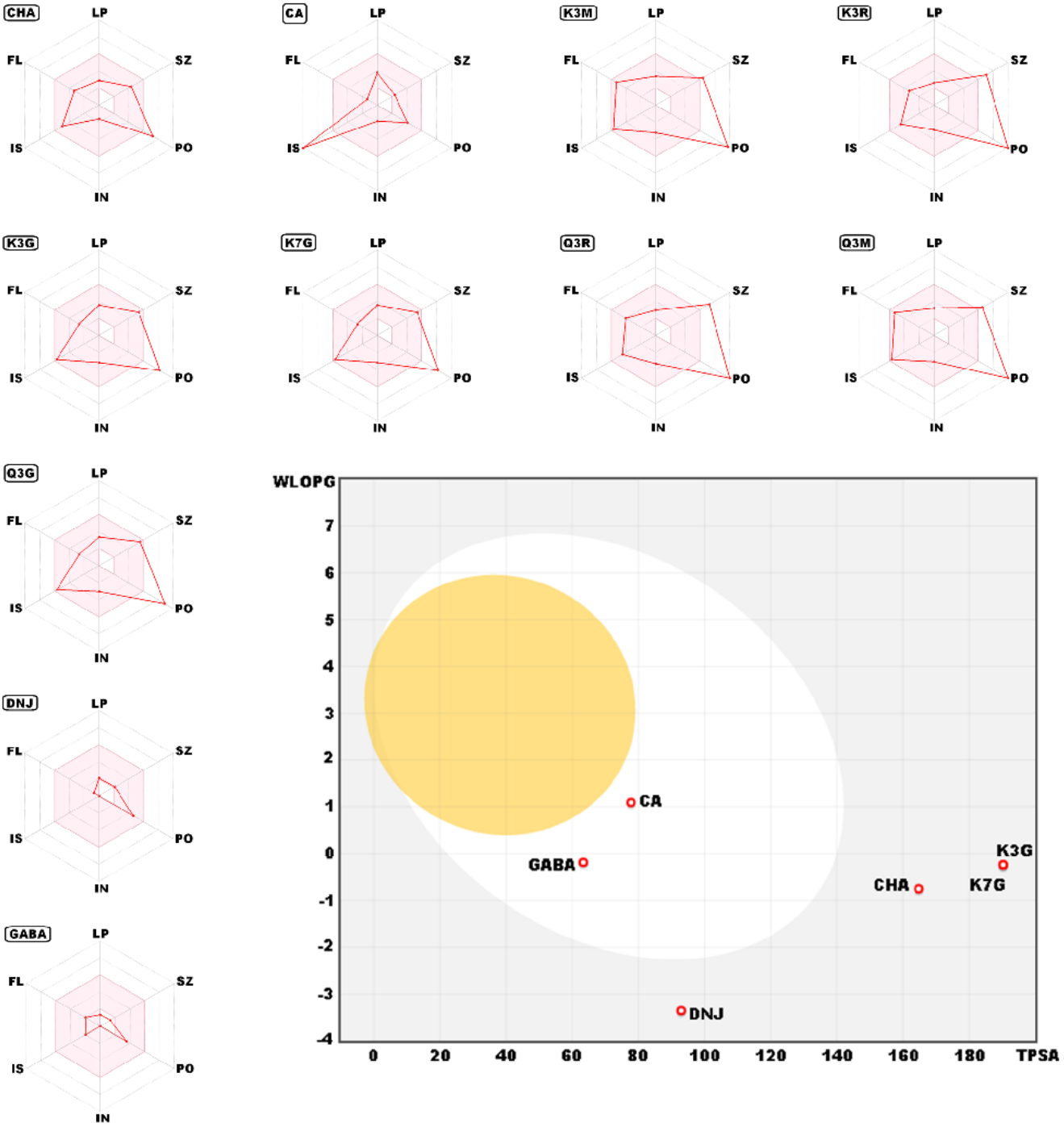

FIGURE 1 Bioavailability radar and prediction of passive human oral-gastrointestinal digestion of nutraceuticals from mulberry leaf extract powders via boiled-egg model. CA, caffeic acid; CHA, chlorogenic acid; DNJ, 1-deoxynojirimycin; FL, flexibility; GABA, gamma-aminobutyric acid; IN, solubility; IS, saturation; K3G, kaempferol-3-glucoside; K3M, kaempferol-3-(6-malonylglucoside); K3R, kaempferol-3-(6-rhamnosylglucoside); K7G-kaempferol-7-O-glucoside; LP, lipophilicity; PO, polarity; Q3G, quercetin-3-O-glucoside; Q3M, quercetin-3-(6-malonylglucoside); Q3R, quercetin-3-rutinose; SZ, size; TPSA, topological polar surface area; WLOG, wildman and crippen atomistic method score

take into consideration probable interactions of biocompounds with the food matrix. Besides, high saturation is related to enhanced absorption which agrees with our results for CA and that exhibited high apparent permeability. Furthermore, the ADMET (Adsorption, distribution, metabolism, excretion, and toxicity) parameters (Table 2) show that the MLEPs nutraceuticals hada high probability of being absorbed and bioavailable.

4 | CONCLUSION

In this research, the release and intestinal absorption mechanisms of nutraceuticals from mulberry leaf extract encapsulated with diverse techniques were investigated using an in vitro stimulated digestion. The mathematical analysis of release models of nutraceuticals from different modalities has evidenced that carrier material

was the main parameter that significantly impact the freeing of nutraceuticals. Albeit diffusion, erosion, and diffusion mechanisms could coexist for the controlled release of mulberry leaf nutraceuticals, the Korsmeyer-Peppas model suggested that mulberry leaf nutraceuticals release was mainly controlled by pseudo-Fickian diffusion (for the unencapsulated sample at gastric phase), Fickian diffusion (for samples encapsulated with maltodextrin at the gastric and intestinal phase), non-Fickian diffusion (for the unencapsulated sample at intestinal stage and samples encapsulated with sodium carboxymethyl cellulose at gastric phase), and case II transport (for samples encapsulated with sodium carboxymethyl cellulose at intestinal phase). The Permeability assays conducted in everted rat sacs revealed that encapsulation decreased the apparent permeability coefficient of nutraceuticals from mulberry leaf extract. Furthermore, the apparent permeability coefficient crossing the everted gut sac of nutraceuticals was higher in encapsulated samples with maltodextrin than those entrapped with CMC, as well as spray dry samples than those of freeze-dry samples.

The information gained in this study gives insight into the effect of encapsulation techniques on the nutraceuticals release and their intestinal permeability, which are a pivotal factor of systemic absorption, which allow us to better assess the potential of encapsulated leaf extract as a functional food ingredient.

AUTHOR CONTRIBUTIONS

William Tchabo: Conceptualization; formal analysis; methodology; software; writing – original draft. **giscard Kuate Kaptso:** Software; writing – original draft. **Guifeng Bao:** Formal analysis. **Kenuo Wang:** Formal analysis. **Newlove A Afoakwah:** Writing – review and editing. **Carl Moses Mbofung:** Conceptualization; data curation; methodology. **Xiangyang Wang:** Conceptualization; supervision; validation.

ACKNOWLEDGMENT

The authors appreciate the valuable contributions of the senior software engineer Robert Patrick Lekane Tchabo of Alfa financial software, London (UK) for providing OriginPro codes for initializing model parameters and the guidance on the non-linear modeling. This research did not receive any specific grant from funding agencies in the public, commercial, or not-for-profit sectors.

CONFLICT OF INTEREST

The authors have declared no conflicts of interest for this article.

DATA AVAILABILITY STATEMENT

Data available on request from the authors.

ORCID

William Tchabo https://orcid.org/0000-0002-4796-3512

REFERENCES

Aguillón-Osma, J., Luzardo-Ocampo, I., Cuellar-Nuñez, M. L., Maldonado-Celis, M. E., Loango-Chamorro, N., & Campos-Vega, R. (2019). Impact of *in vitro* gastrointestinal digestion on the bioaccessibility and antioxidant capacity of bioactive compounds from passion fruit (*Passiflora edulis*) leaves and juice extracts. *Journal of Food Biochemistry*, *43*, e12879.

Bacaita, E. S., Ciobanu, B. C., Popa, M., Agop, M., & Desbrieres, J. (2014). Phases in the temporal multiscale evolution of the drug release mechanism in IPN-type chitosan based hydrogels. *Physical Chemistry Chemical Physics*, *16*, 25896–25905.

Berkane, E., Orlik, F., Charbit, A., Danelon, C., Fournier, D., Benz, R., & Winterhalter, M. (2005). Nanopores: Maltoporin channel as a sensor for maltodextrin and lambda-phage. *Journal of Nanobiotechnology*, *3*, 3.

Bhushani, J. A., Kurrey, N. K., & Anandharamakrishnan, C. (2017). Nanoencapsulation of green tea catechins by electrospraying technique and its effect on controlled release and in-vitro permeability. *Journal of Food Engineering*, *199*, 82–92.

Caicedo-Lopez, L. H., Luzardo-Ocampo, I., Cuellar-Nuñez, M. L., Campos-Vega, R., Mendoza, S., & Loarca-Piña, G. (2019). Effect of the *in vitro* gastrointestinal digestion on free-phenolic compounds and mono/oligosaccharides from *Moringa oleifera* leaves: Bioaccessibility, intestinal permeability and antioxidant capacity. *Food Research International*, *120*, 631–642.

Çam, M., İçyer, N. C., & Erdoğan, F. (2014). Pomegranate peel phenolics: Microencapsulation, storage stability and potential ingredient for functional food development. *LWT-Food Science and Technology*, *55*, 117–123.

Campos-Vega, R., Vázquez-Sánchez, K., López-Barrera, D., Loarca-Piña, G., Mendoza-Díaz, S., & Oomah, B. D. (2015). Simulated gastrointestinal digestion and *in vitro* colonic fermentation of spent coffee (*Coffea arabica* L.): Bioaccessibility and intestinal permeability. *Food Research International*, *77*, 156–161.

Costamagna, M. S., Gómez-Mascaraque, L. G., Zampini, I. C., Alberto, M. R., Pérez, J., López-Rubio, A., & Isla, M. I. (2017). Microencapsulated chañar phenolics: A potential ingredient for functional foods development. *Journal of Functional Foods*, *37*, 523–530.

Dhiman, S., Kumar, V., Mehta, C. M., Gat, Y., & Kaur, S. (2020). Bioactive compounds, health benefits and utilisation of *Morus* spp. – A comprehensive review. *The Journal of Horticultural Science and Biotechnology*, *95*, 8–18.

Díaz-Bandera, D., Villanueva-Carvajal, A., Dublán-García, O., Quintero-Salazar, B., & Dominguez-Lopez, A. (2015). Assessing release kinetics and dissolution of spray-dried Roselle (*Hibiscus sabdariffa* L.) extract encapsulated with different carrier agents. *LWT-Food Science and Technology*, *64*, 693–698.

Espinosa-Páez, E., Hernández-Luna, C. E., Longoria-García, S., Martínez-Silva, P. A., Ortiz-Rodríguez, I., Villarreal-Vera, M. T., & Cantú-Saldaña, C. M. (2021). *Pleurotus ostreatus*: A potential concurrent biotransformation agent/ingredient on development of functional foods (cookies). *LWT*, *148*, 111727.

Feng, J., Wu, Y., Zhang, L., Li, Y., Liu, S., Wang, H., & Li, C. (2019). Enhanced chemical stability, intestinal absorption, and intracellular antioxidant activity of Cyanidin-3-O-glucoside by composite nanogel encapsulation. *Journal of Agricultural and Food Chemistry*, *67*, 10432–10447.

Flores, F. P., & Kong, F. (2017). In vitro release kinetics of microencapsulated materials and the effect of the food matrix. *Annual Review of Food Science and Technology*, *8*, 237–259.

González, E., Gómez-Caravaca, A. M., Giménez, B., Cebrián, R., Maqueda, M., Parada, J., Martínez-Férez, A., Segura-Carretero, A., & Robert, P. (2020). Role of maltodextrin and inulin as encapsulating agents on the protection of oleuropein during *in vitro* gastrointestinal digestion. *Food Chemistry*, *310*, 125976.

González, F., García-Martínez, E., del Mar Camacho, M., Martínez-Navarrete, N., Sarmento, B., Fernandes, I., Freitas, V., Rodrigues, F., & Oliveira, B. (2019). Insights into the development of grapefruit nutraceutical powder by spray drying: Physical characterization, chemical composition and 3D intestinal permeability. *Journal of the Science of Food and Agriculture*, *99*, 4686–4694.

He, X., Chen, X., Ou, X., Ma, L., Xu, W., & Huang, K. (2020). Evaluation of flavonoid and polyphenol constituents in mulberry leaves using HPLC fingerprint analysis. *International Journal of Food Science & Technology*, *55*, 526–533.

Heep, G., Almeida, A., Marcano, R., Vieira, D., Mainardes, R. M., Khalil, N. M., & Sarmento, B. (2019). Zein-casein-lysine multicomposite nanoparticles are effective in modulate the intestinal permeability of ferulic acid. *International Journal of Biological Macromolecules*, *138*, 244–251.

Herrera-Cazares, L. A., Hernández-Navarro, F., Ramírez-Jiménez, A. K., Campos-Vega, R., de la Luz Reyes-Vega, M., Loarca-Piña, G., Morales-Sánchez, E., Wall-Medrano, A., & Gaytán-Martínez, M. (2017). Mango-bagasse functional-confectionery: Vehicle for enhancing bioaccessibility and permeability of phenolic compounds. *Food & Function*, *8*, 3906–3916.

Kanha, N., Regenstein, J. M., Surawang, S., Pitchakarn, P., & Laokuldilok, T. (2021). Properties and kinetics of the *in vitro* release of anthocyanin-rich microcapsules produced through spray and freeze-drying complex coacervated double emulsions. *Food Chemistry*, *340*, 127950.

Kavousi, H. R., Fathi, M., & Goli, S. A. H. (2018). Novel cress seed mucilage and sodium caseinate microparticles for encapsulation of curcumin: An approach for controlled release. *Food and Bioproducts Processing*, *110*, 126–135.

Kullman, L., Winterhalter, M., & Bezrukov, S. M. (2002). Transport of maltodextrins through Maltoporin: A single-channel study. *Biophysical Journal*, *82*, 803–812.

Luzardo-Ocampo, I., Campos-Vega, R., Gaytán-Martínez, M., Preciado-Ortiz, R., Mendoza, S., & Loarca-Piña, G. (2017). Bioaccessibility and antioxidant activity of free phenolic compounds and oligosaccharides from corn (*Zea mays* L.) and common bean (*Phaseolus vulgaris* L.) chips during *in vitro* gastrointestinal digestion and simulated colonic fermentation. *Food Research International*, *100*, 304–311.

Luzardo-Ocampo, I., Ramírez-Jiménez, A. K., Cabrera-Ramírez, Á. H., Rodríguez-Castillo, N., Campos-Vega, R., Loarca-Piña, G., & Gaytán-Martínez, M. (2020). Impact of cooking and nixtamalization on the bioaccessibility and antioxidant capacity of phenolic compounds from two sorghum varieties. *Food Chemistry*, *309*, 125684.

Madene, A., Jacquot, M., Scher, J., & Desobry, S. (2006). Flavour encapsulation and controlled release - A review. *International Journal of Food Science & Technology*, *41*, 1–21.

Malekjani, N., & Jafari, S. M. (2020). Release modeling of nanoencapsulated food ingredients by empirical and semiempirical models. In *Release and bioavailability of nanoencapsulated food ingredients* (pp. 211–246). Academic Press.

Papadopoulou, V., Kosmidis, K., Vlachou, M., & Macheras, P. (2006). On the use of the Weibull function for the discernment of drug release mechanisms. *International Journal of Pharmaceutics*, *309*, 44–50.

Pasrija, D., Ezhilarasi, P., Indrani, D., & Anandharamakrishnan, C. (2015). Microencapsulation of green tea polyphenols and its effect on incorporated bread quality. *LWT-Food Science and Technology*, *64*, 289–296.

Pereira Camelo, S. R., Franceschi, S., Perez, E., Girod Fullana, S., & Ré, M. I. (2016). Factors influencing the erosion rate and the drug release kinetics from organogels designed as matrices for oral controlled release of a hydrophobic drug. *Drug Development and Industrial Pharmacy*, *42*, 985–997.

Pérez-Sánchez, A., Borrás-Linares, I., Barrajón-Catalán, E., Arráez-Román, D., González-Álvarez, I., Ibáñez, E., Segura-Carretero, A., Bermejo, M., & Micol, V. (2017). Evaluation of the intestinal permeability of rosemary (*Rosmarinus officinalis* L.) extract polyphenols and terpenoids in Caco-2 cell monolayers. *PLOS ONE*, *12*, e0172063.

Quilaqueo, M., Millao, S., Luzardo-Ocampo, I., Campos-Vega, R., Acevedo, F., Shene, C., & Rubilar, M. (2019). Inclusion of piperine in β-cyclodextrin complexes improves their bioaccessibility and *in vitro* antioxidant capacity. *Food Hydrocolloids*, *91*, 143–152.

Radić, K., Jurišić Dukovski, B., & Vitali Čepo, D. (2020). Influence of pomace matrix and cyclodextrin encapsulation on olive pomace Polyphenols' bioaccessibility and intestinal permeability. *Nutrients*, *12*, 669.

Rastogi, H., & Jana, S. (2016). Evaluation of physicochemical properties and intestinal permeability of six dietary polyphenols in human intestinal colon adenocarcinoma Caco-2 cells. *European Journal of Drug Metabolism and Pharmacokinetics*, *41*, 33–43.

Rezaei, A., Nasirpour, A., Tavanai, H., & Fathi, M. (2016). A study on the release kinetics and mechanisms of vanillin incorporated in almond gum/polyvinyl alcohol composite nanofibers in different aqueous food simulants and simulated saliva. *Flavour and Fragrance Journal*, *31*, 442–447.

Serrano-Cruz, M. R., Villanueva-Carvajal, A., Rosales, E. J. M., Dávila, J. F. R., & Dominguez-Lopez, A. (2013). Controlled release and antioxidant activity of Roselle (*Hibiscus sabdariffa* L.) extract encapsulated in mixtures of carboxymethyl cellulose, whey protein, and pectin. *LWT-Food Science and Technology*, *50*, 554–561.

Shen, X., Zhao, C., Lu, J., & Guo, M. (2018). Physicochemical properties of whey-protein-stabilized astaxanthin Nanodispersion and its transport via a Caco-2 monolayer. *Journal of Agricultural and Food Chemistry*, *66*, 1472–1478.

Tchabo, W., Ma, Y., Kaptso, G. K., Kwaw, E., Cheno, R. W., Wu, M., Osae, R., Ma, S., & Farooq, M. (2018). Carrier effects on the chemical and physical properties of freeze-dried encapsulated mulberry leaf extract powder. *Acta Chimica Slovenica*, *65*, 823–835.

Tchabo, W., Ma, Y., Kaptso, G. K., Kwaw, E., Cheno, R. W., Xiao, L., Osae, R., Wu, M., & Farooq, M. (2019). Process analysis of mulberry (*Morus alba*) leaf extract encapsulation: Effects of spray drying conditions on bioactive encapsulated powder quality. *Food and Bioprocess Technology*, *12*, 122–146.

Tchabo, W., Ma, Y., Kwaw, E., Xiao, L., Wu, M., & Maurice, A. T. (2018). Impact of extraction parameters and their optimization on the nutraceuticals and antioxidant properties of aqueous extract mulberry leaf. *International Journal of Food Properties*, *21*, 717–732.

Tian, X.-J., Yang, X.-W., Yang, X., & Wang, K. (2009). Studies of intestinal permeability of 36 flavonoids using Caco-2 cell monolayer model. *International Journal of Pharmaceutics*, *367*, 58–64.

Trevisol, T. C., Scartazzini, L., Valério, A., Ulson, G., de Souza, S. M. A., Bierhalz, A. C. K., & Valle, J. A. B. (2020). Diclofenac release from alginate/carboxymethyl cellulose mono and bilayer films for wound dressing applications. *Cellulose*, *27*, 6629–6642.

Villela-Castrejón, J., Antunes-Ricardo, M., & Gutiérrez-Uribe, J. A. (2017). Bioavailability and anti-inflammatory activity of phenolic acids found in spray-dried nejayote after its *in vitro* digestion. *Journal of Functional Foods*, *39*, 37–43.

Wen, P., Hu, T.-G., Linhardt, R. J., Liao, S.-T., Wu, H., & Zou, Y.-X. (2019). Mulberry: A review of bioactive compounds and advanced processing technology. *Trends in Food Science & Technology*, *83*, 138–158.

Zokti, J. A., Sham Baharin, B., Mohammed, A. S., & Abas, F. (2016). Green tea leaves extract: Microencapsulation, physicochemical and storage stability study. *Molecules*, *21*, 940.

SUPPORTING INFORMATION

Additional supporting information may be found in the online version of the article at the publisher's website.

How to cite this article: Tchabo, W., Kaptso, G. K., Bao, G., Wang, K., Afoakwah, N. A., Mbofung, C. M., Wang, X. (2022). Impact of encapsulation techniques (drying methods and carrier materials) on the nutraceuticals release and absorption mechanism of mulberry leaf. *Journal of Food Processing and Preservation*, *46*, e16730. https://doi.org/10.1111/jfpp.16730